

# Temperature-dependent Nucleation and Growth of Dendrite-Free Lithium Metal Anodes

Kang Yan, Jiangyan Wang, Shuoqing Zhao, Dong Zhou, Bing Sun,\* Yi Cui,\* and Guoxiu Wang\*

**Abstract:** It is essential to develop a facile and effective method to enhance the electrochemical performance of lithium metal anodes for building high-energy-density Li-metal based batteries. Herein, we explored the temperature-dependent Li nucleation and growth behavior and constructed a dendrite-free Li metal anode by elevating temperature from room temperature (20°C) to 60°C. A series of ex situ and in situ microscopy investigations demonstrate that increasing Li deposition temperature results in large nuclei size, low nucleation density, and compact growth of Li metal. We reveal that the enhanced lithiophilicity and the increased Li-ion diffusion coefficient in aprotic electrolytes at high temperature are essential factors contributing to the dendrite-free Li growth behavior. As anodes in both half cells and full cells, the compact deposited Li with minimized specific surface area delivered high Coulombic efficiencies and long cycling stability at 60°C.

It is widely recognized that lithium-based batteries including Li metal-ion, Li-sulfur and Li-air batteries are promising next generation batteries, owing to their ultra-high capacities and energy densities.<sup>[1]</sup> Significant progress has been achieved on sulfur cathodes since the Li-sulfur batteries with super high capacities were reported in 2009.<sup>[2]</sup> New materials are also explored for high-performance oxygen cathode of Li-air batteries.<sup>[3]</sup> The performances of both Li-sulfur and Li-air batteries significantly depend on Li metal anodes. However, the research on Li metal anode only started to flourish over the past five years.<sup>[4]</sup> Dendrite-free Li metal anodes with high Coulombic efficiencies are the ultimate goal to achieve high-energy-density Li metal batteries. It was widely recognized

that partial strong electric field leads to non-uniform Li ion distribution thus resulting in dendrite generation. Therefore, reducing local current density by increasing the surface area of current collector is a popular strategy to suppress Li dendrite.<sup>[5]</sup> Moreover, considerable approaches have been developed to suppress Li dendrite formation during repeated plating/stripping process. These include surface protective layer,<sup>[6]</sup> large area conductive/non-conductive hosts<sup>[7]</sup> and novel ion refluxing structures.<sup>[8]</sup> However, the formation and growth mechanisms of Li dendrite are still intricate and obscure due to many factors in the complex battery system. Although previous investigations probed Li dendrite growth regarding various factors,<sup>[9]</sup> the common factor of temperature is seldom studied in the spectrum of dendrite formation. Apart from consumer electronics that work at room temperature, emerging applications expect batteries to operate under thermal extremes. As the choice of anodes in next generation high-energy-density batteries, Li metal anode requires the critical examination on its thermal characteristics.

Herein, we revealed the dramatic changes of Li nucleation and growth behavior under the influence of operation temperatures. Enhanced lithiophilicity and rapid Li ion migration induced by the increase of temperature contributed to large nuclei size and small nucleation density, which resulted in uniform and compact Li deposition. We further demonstrated that the differences of Li nucleation behaviors originate from the onsets of Li nuclei formation via in situ optical microscope observation. At 60°C, the formation of Li dendrite was effectively suppressed and the solid electrolyte interface (SEI) was stabilized, the corresponding Li || Cu half cells and Li || Li<sub>4</sub>Ti<sub>5</sub>O<sub>12</sub> (LTO) full cells achieved extended life-spans and increased Coulombic efficiencies.

We first elucidated the differences of Li nuclei layers at various temperatures and current densities using Li || Cu half cells in ether-based electrolyte (1M lithium bis (trifluoromethanesulfonyl)imide (LiTFSI) in 1,3-dioxolane/1,2-dimethoxyethane (DOL/DME, 1:1 v/v) with 1 wt % LiNO<sub>3</sub>). To investigate the morphologies of Li nuclei layers, a fixed areal capacity of 0.1 mA h cm<sup>-2</sup> was used, which exactly fulfilled the initial Li nucleation processes. As shown in scanning electron microscope (SEM) images (Figure 1) and statistic histograms (Figure S1 in the Supporting Information), Li nuclei size decreases significantly and Li nucleation density increases remarkably with the increase of current density at the fixed temperature, which is well consistent with previous research.<sup>[9a]</sup> Notably, we discovered a thermal-phenomena pertaining to Li nucleation behavior. By elevating temperature from -20°C to 60°C, the Li nuclei show enlarged size and decreased density at the same current density. For

[\*] K. Yan, S. Zhao, Dr. D. Zhou, Dr. B. Sun, Prof. G. Wang  
Centre for Clean Energy Technology  
School of Mathematical and Physical Sciences, Faculty of Science  
University of Technology Sydney  
Sydney, NSW 2007 (Australia)  
E-mail: bing.sun@uts.edu.au  
guoxiu.wang@uts.edu.au

Dr. J. Wang, Prof. Y. Cui  
Department of Materials Science and Engineering  
Stanford University  
Stanford, CA 94305 (USA)

Prof. Y. Cui  
SLAC National Accelerator Laboratory  
Stanford Institute for Materials and Energy Sciences  
2575 Sand Hill Road, Menlo Park, CA 94025 (USA)  
E-mail: yicui@stanford.edu

Supporting information and the ORCID identification number(s) for the author(s) of this article can be found under:  
<https://doi.org/10.1002/anie.201905251>.

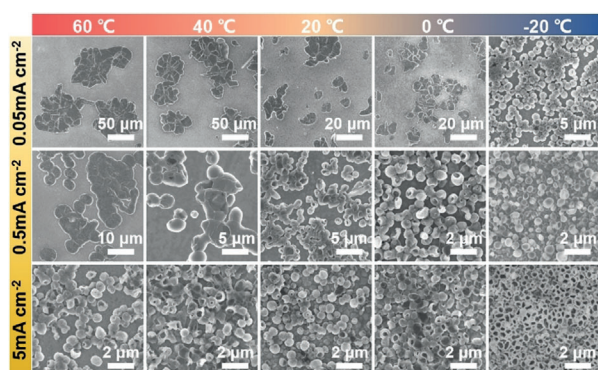


**Figure 1.** SEM images of Li nuclei layers at varied current densities and temperature conditions with the capacity limitation of  $0.1 \text{ mAh cm}^{-2}$ .

instance, at the current density of  $0.05 \text{ mA cm}^{-2}$ , Li nuclei are discrete and compact at  $60^\circ\text{C}$  (Figure 1). While at  $20^\circ\text{C}$ , Li nuclei become smaller and denser. As the temperature further decreases to  $-20^\circ\text{C}$ , the Li nuclei become even smaller and more crowded. The statistic histograms more clearly elucidate the dramatic changes of Li nuclei size and nucleation density (Figure 2a). At  $0.05 \text{ mA cm}^{-2}$  and  $-20^\circ\text{C}$ , the Li nuclei size and nuclei density are  $1.4 \mu\text{m}$  and  $4.0 \times 10^6 \text{ nuclei cm}^{-2}$ , respectively. In contrast, the nuclei size increases twenty times and the nucleation density drops to one percent as temperature increases from  $-20^\circ\text{C}$  to  $60^\circ\text{C}$ . The same tendencies were also observed when we varied the current density (Figure S2). Upon the systematical ex situ SEM observations, we identified that high temperature favored large and sparse Li nuclei formation. In carbonate electrolyte (1M LiPF<sub>6</sub> in ethylene carbonate/dimethyl carbonate (EC/DMC, 1:1 v/v)), we also observed Li deposition layer

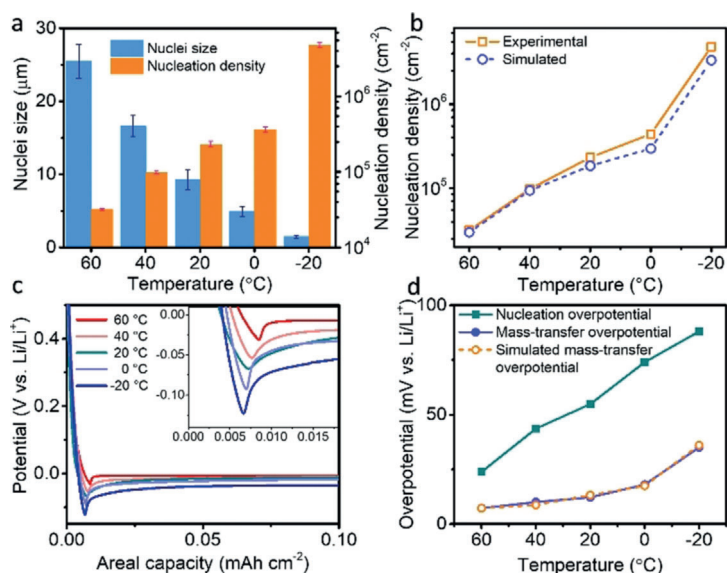


**Figure 2.** a) Statistic histograms of Li nuclei size and nucleation density for Li plating at  $0.05 \text{ mA cm}^{-2}$ . b) Change in Li nucleation densities with temperature. c) Chronoamperometric comparison of Li nucleation at varied temperature at  $0.05 \text{ mA cm}^{-2}$ . d) Change in nucleation overpotentials and experimental and simulated mass-transfer overpotentials with temperature.

became more compact at higher temperature (Figure S3), indicating the universal influence of temperature on Li nucleation behavior.

As a conventional method for quantifying electrochemical nucleation, chronoamperometry has been used to model heterogeneous nucleation behavior.<sup>[10]</sup> Therefore, we further investigated Li nucleation density under the influence of temperature by chronoamperometry measurements. Typical Li nucleation curves were obtained by employing three different onset potentials that correspond to three deposition current densities ( $0.05$ ,  $0.5$  and  $5 \text{ mA cm}^{-2}$ ; Figure S4). The well-defined proportional trend between the current ( $I$ ) and the root of time ( $t^{1/2}$ ) illustrated that Li nucleation behavior followed three-dimensional instantaneous model (Figure S5).<sup>[11]</sup> In order to eliminating systemic deviation that caused by diffusion gradient, we did simulation by introducing diffusion coefficient and slope value of  $I-t^{1/2}$  curve into nucleation model at a low current density ( $0.05 \text{ mA cm}^{-2}$ ). The detailed modeling and simulation are described in the supporting information. As shown in Figure 2b, nucleation densities obtained from both experimental statistic and model simulation decrease dramatically with increasing temperature, clearly proving the degressive Li nucleation density at ascending temperature.

Chronopotentiometry measurements were also conducted to evaluate Li nucleation property. All the voltage–capacity profiles exhibit voltage dips at the beginning of Li nucleation which followed by voltage plateaus (Figure 2c). The value between the bottom of voltage dip and the flat part of voltage plateau represents the Li nucleation overpotential, which identifies the degree of lithiophilicity on the current collector surface.<sup>[12]</sup> Li nucleation overpotential significantly decreased as the temperatures increased from  $-20^\circ\text{C}$  to  $60^\circ\text{C}$ , illustrating the lowest nucleation energy barrier and the best lithiophilicity at  $60^\circ\text{C}$ . Furthermore, the plateaus depict the mass-transfer overpotential, which are mainly determined by the current density and the migration properties of Li ions in electrolyte. The lowest mass-transfer overpotential was found at  $60^\circ\text{C}$  at the same current density, indicating the facile Li nucleation growth process at high temperature. The enhanced lithiophilicity facilitated the formation of Li embryos on current collector, and the depressed mass-transfer overpotential further strengthened the nuclei growth, thus contributing to large Li nuclei size at elevated temperature. In addition, the decreasing tendencies of nucleation overpotential and mass-transfer overpotential with increasing temperature were well demonstrated by simulations (Figure 2d, Figure S6,S7), illustrating large Li nuclei induced by thermal elevation.

To better understand the mechanism of Li nuclei layer changes, we conducted in situ optical observation to visualize the critical Li crystallization and nucleation processes. Figure 3a and Supporting Videos S1, S2 show the in vivo Li nucleation growth processes at  $60^\circ\text{C}$  and  $20^\circ\text{C}$  at the same current density ( $0.5 \text{ mA cm}^{-2}$ ). The videos display that numerous Li embryos emerged within transient time (ca.

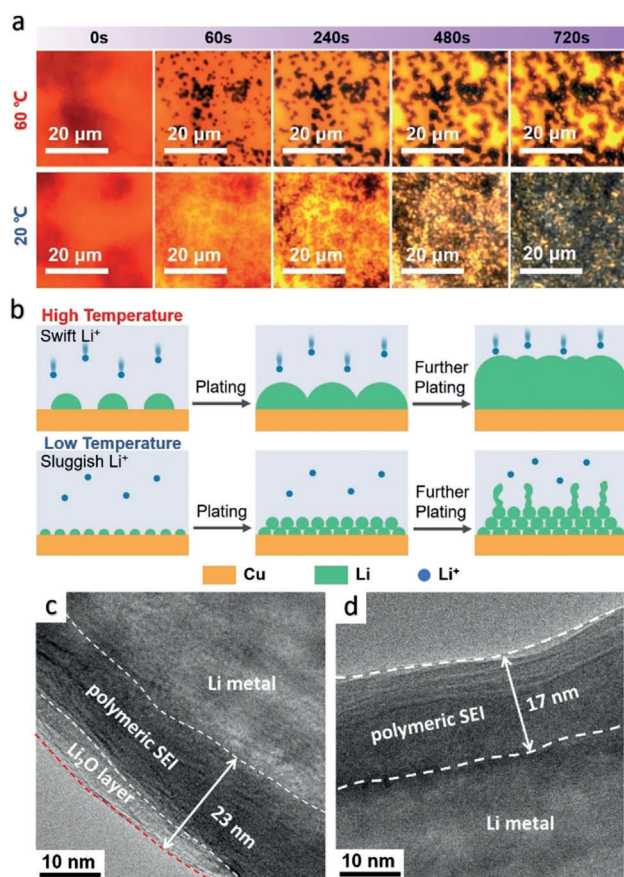


**Figure 3.** a) In situ optical snap images of Li nuclei growth at 60°C and 20°C. b) Schematic illustration of proposed Li nuclei generation and growth mechanism. Cryo-EM images of SEI formed at c) 60°C and d) 20°C.

10 s) at both 60°C and 20°C, clearly certifying the instantaneous nucleation procedure as predicted by previous investigations.<sup>[13]</sup> In the video S1 and S2, Li nuclei generated concurrently as the plating profile passed the voltage dip, indicating the necessary overpotential of metallic Li heterogeneous deposition. The following voltage plateau signified Li nuclei growth, which was clearly revealed by the gradual accretion on Li nuclei size. Larger and sparser Li nuclei were observed at 60°C compared with that at 20°C from the snap image at 60 s (Figure 3a). At 60°C, large Li nuclei gradually grew up and expanded, and large amounts of interspaces were still visible at 720 s. Although the growth of Li nuclei was distinct at 20°C, the nuclei overlaps were clearly observed after 480 s. In situ optical observations successfully correlate SEM observation and simulation analysis, demonstrating that the discriminations of Li nucleation were influenced by temperature from the very beginning.

Accordingly, we proposed the temperature-dependent Li nucleation and growth mechanism. As shown in the schematics (Figure 3b), excellent lithiophilicity promotes interactions between Li ions in electrolyte and current collector at elevated temperature (e.g. 60°C). This effect leads to the gathering of large amount of Li ions on the surface of current collector, thus resulting in large Li nuclei formation in the

initial stage. Meanwhile, the high mobility of Li ions ensures swift migration to the separated Li nuclei points. As plating continues, large and sparse Li nuclei grow gradually until they fuse with their neighbors. Ultimately, a compact Li deposition layer forms after further plating. In contrast, at room temperature (e.g. 20°C), the contact between Li ions and current collector is weakened by poor lithiophilicity. Therefore, small Li nuclei are generated because limited Li ions gather simultaneously. Meanwhile, sluggish mobility of Li ions contributes to dense Li nuclei because Li ions are easily captured by nearby nuclei points. Inevitably, further Li deposition easily results in the overlap of Li nuclei and the generation of Li dendrites. Notably, the Li ions diffusion coefficients are greatly increased at elevated temperature (Figure S8). The Li ions diffusion coefficient at 60°C ( $1.05 \times 10^{-5} \text{ cm}^{-2} \text{ s}^{-1}$ ) shows 3 times higher than that at 20°C ( $3.4 \times 10^{-6} \text{ cm}^{-2} \text{ s}^{-1}$ ), and 17 times higher than that at -20°C ( $6.1 \times 10^{-7} \text{ cm}^{-2} \text{ s}^{-1}$ ). The migration of Li ions through SEI is also promoted according to the significant decrease of charge transfer resistance ( $R_{ct}$ ) with the increase of temperature (Figure S9, Table S3). Furthermore, the strengthened Li ion de-solvation ability at high temperature has been demonstrated.<sup>[14]</sup> As a result, fast Li ions diffusion and migration abilities and enhanced Li ion de-solvation performance synergistically contribute to large and sparse Li nuclei generation and compact Li deposition layer formation. This strongly supports the temperature-dependent Li nucleation and growth mechanism.

For further investigation, the Li deposition layers with high areal capacities at different temperatures were systematically observed (Figure S10–S13). At 60°C, the compact and smooth lithium layer was found at  $0.5 \text{ mA cm}^{-2}$  with the areal capacity of  $1 \text{ mAh cm}^{-2}$ . Large area of blank Cu foil surface was still visible among Li agglomerates (Figure S10). This confirmed that compact and packed Li occupied minimal space and possessed very low surface area which minimized SEI formation. After increasing the areal capacities, similar lithium layers were also observed except the hiding of blank Cu foil (Figure S11). By contrast, the Li deposition layer formed at 20°C consisted of large amount of twisted dendritic Li as well as massive interspaces. When the temperature down to -20°C, thick Li dendrites and more vacancies were observed on Li deposition layer. The porous and dendritic Li deposition layers induce increased consumption of electrolyte and Li due to the SEI formation at 20°C and -20°C. Note, the obvious changes of component and nanostructure of SEI layers at varied temperatures were clearly demonstrated using Cryo-EM characterization (Figure 3c,d). The SEI formed at 20°C was an amorphous polymeric interphase, while the SEI formed at 60°C consisted of an amorphous polymeric interphase and an inorganic Li<sub>2</sub>O outer layer. In addition, the thickness of SEI layer increases from 17 nm at 20°C to 23 nm at 60°C.

To evaluate the electrochemical performances of Li anodes at varied temperatures, we tested the Li||Cu half cells at  $0.5 \text{ mA cm}^{-2}$  with the areal capacity of  $1 \text{ mAh cm}^{-2}$  (Figure 4a). A quadruple enhancement of cyclability was obtained by increasing the temperature from 20°C to 60°C, and the average Coulombic efficiency at 60°C was amelio-

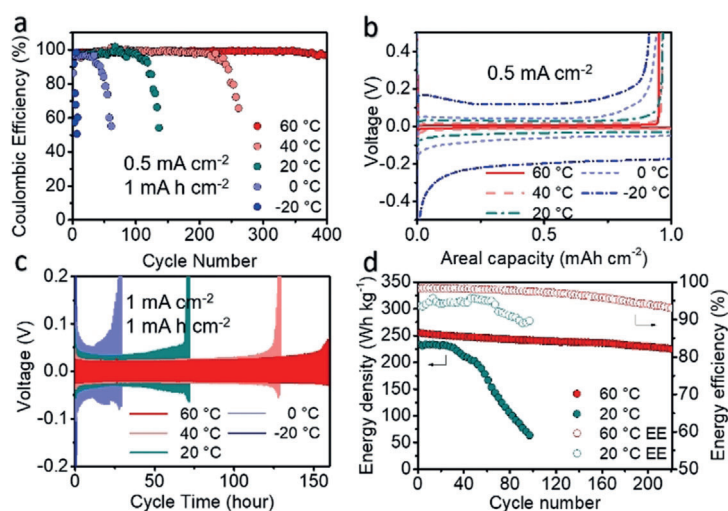


**Figure 4.** a) Coulombic efficiencies of Li plating/stripping on Cu at different temperatures. b) The first cycle voltage profiles of Li plating/stripping. c) Charge/discharge voltage profiles of Li||Li symmetric cells. d) Energy density and energy efficiency of Li||LTO full cells at 60°C and 20°C.

rated to 98.9% from that of 97.7% at 20°C. Furthermore, the electrochemical performance improvements of half cells led by temperature elevation showed similar trends at larger current densities and higher areal capacities (Figure S14 and S15). Apart from the compact and uniform texture of Li deposition layer, the high Coulombic efficiency and long cycling life at high temperature were further warranted by the thicker multilayered SEI formed at 60°C, since the stable Li<sub>2</sub>O layer more effectively passivated the anode. The corresponding voltage profiles showed reduced overpotentials during Li plating/stripping at elevated temperature (Figure 4b and Figure S16), which was attributed to the enhanced Li ion migration ability and reduced electrolyte resistance at high temperature.

The influence of temperature on the electrochemical behaviors of Li anodes were further evaluated using Li||Li symmetric cells. In Figure 4c, the symmetric cells operated at 60°C exhibits long life span, which is more than double of that at 20°C. The lowest overpotential and the best cyclability were also achieved at different current densities at 60°C (Figure S17). The significantly improved electrochemical performances of symmetric cells at elevated temperature are consistent with the results of Li||Cu half cells. In general, low Coulombic efficiency and poor cyclability of Li anodes are caused by the formation of SEI and the accumulation of “dead” Li upon cycling. Based on the above testing results, we confirm that high temperature benefits reversible Li plating/stripping, retards the side reaction of SEI formation and effectively suppresses the accumulation of “dead” Li.

As a proof of concept, we assembled Li||Li<sub>4</sub>Ti<sub>5</sub>O<sub>12</sub> (LTO) full cells to examine their thermal characteristics. The anodes were employed by pre-depositing Li on Cu foil with a fixed capacity of 5 mA h cm<sup>-2</sup>. The full cells were tested at 0.5 mA cm<sup>-2</sup> at 60°C and 20°C, respectively. In Figure 4d, the initial discharge energy densities of full cells were improved from 233 Wh kg<sup>-1</sup> to 255 Wh kg<sup>-1</sup> as the operation

temperature increased from 20°C to 60°C. Furthermore, the cycle life of full cell was significantly prolonged, and the energy efficiency was distinctly enhanced at 60°C. The improved energy density at high temperature was contributed by the reduced discharge overpotentials and increased discharge specific capacity (Figure S18 and S19). Considering that a novel effective device has been reported to improve the performances of batteries at low temperature,<sup>[15]</sup> we demonstrate the practicability of promoting the performances of Li metal-based full cells efficiently at high temperature.

In conclusion, we discovered the crucial impact of temperature on the nucleation behavior and electrochemical performance of Li metal anodes. Ex situ and in situ microscope observations clearly demonstrated that larger Li nuclei with smaller nucleation density formed on Cu foil at higher temperature. The enhanced lithiophilicity and Li-ion migration ability at elevated temperature were shown to facilitate the formation of large nuclei size with small nucleation density. Moreover, we obtained dendrite-free Li deposition layers with an areal capacity as high as 5 mA h cm<sup>-2</sup> at 60°C. The Li||Cu half cells and Li||Li symmetric cells exhibited long cyclability, high Coulombic efficiency, and low overpotential at high temperature. In addition, Li||LTO full cells delivered outstanding performances at 60°C, which greatly surpassed that of the full cells at 20°C. Therefore, elevating temperature has been proved to be an efficient and facile method for developing high-performance Li metal-based batteries. This strategy may also be extended for preventing dendrite growth in other rechargeable metal-based batteries.

### Acknowledgements

We gratefully acknowledge the financial support by Australian Research Council (ARC) through ARC Discovery Project (DP160104340 and DP170100436) and ARC Discovery Early Career Researcher Award (DE180100036). We thank Linda Xiao for her kind help on microscope operation. K.Y. thanks the financial support from the China Scholarship Council (No. 201606030088).

### Conflict of interest

The authors declare no conflict of interest.

**Keywords:** dendrite-free · ion migration · Li metal anodes · nucleation and growth · temperature-dependent behavior

[1] a) J. Liu, Z. Bao, Y. Cui, E. J. Dufek, J. B. Goodenough, P. Khalifah, Q. Li, B. Y. Liaw, P. Liu, A. Manthiram, Y. S. Meng, V. R. Subramanian, M. F. Toney, V. V. Viswanathan, M. S.

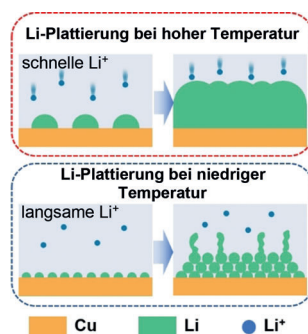


## Zuschriften

## Lithiumbatterien

K. Yan, J. Wang, S. Zhao, D. Zhou,  
B. Sun,\* Y. Cui,\*  
G. Wang\* ————— ■■■■-■■■■

Temperature-dependent Nucleation and  
Growth of Dendrite-Free Lithium Metal  
Anodes



**Elektrodenplattierung:** Starke Lithiophilie und schnelle Li<sup>+</sup>-Wanderung bei erhöhter Temperatur ermöglichen die Bildung großer, verstreuter Li-Keime und liefern damit einen Beitrag zu einer kompakten und glatten Li-Abscheidungsschicht auf Anoden. So konnten dendritfreie Li-Metallanoden mit exzellenter elektrochemischer Leistung für metallbasierte Batterien erzielt werden.